atmosphere

MDPI

Article

Spatiotemporal Trends and Influencing Factors of $PM_{2.5}$ Concentration in Eastern China from 2001 to 2018 Using Satellite-Derived High-Resolution Data

Weihang Wang, Qingqing He *, Kai Gao, Ming Zhang and Yanbin Yuan

School of Resource and Environmental Engineering, Wuhan University of Technology, Wuhan 430070, China
* Correspondence: qqhe@whut.edu.cn; Tel.: +86-27-68758403

Abstract: Ambient exposure to fine particulate matter ($PM_{2.5}$) in eastern China, a densely populated region with very high-level $PM_{2.5}$ pollution, has attracted great concern from the public, government, and scientific community. By taking advantage of advanced statistical methods and a high-resolution $PM_{2.5}$ dataset, this study explicitly investigated the spatiotemporal changes in $PM_{2.5}$ in eastern China from 2001 to 2018 at multiple spatial and temporal scales and examined its links with natural and socioeconomic factors to explore their effects on $PM_{2.5}$ changes. This study found that the $PM_{2.5}$ concentration in most of eastern China declined recently, while most of the discernable decreasing trends occurred in the southern and western areas of the study domain, and the statistically significant increasing trends were primarily in the North China Plain. The influencing factors analysis found that, among the selected four natural and five anthropogenic factors, temperature, and population density exerted more potent effects than the other influencing factors, and all the influencing factors were found to impose complex effects on the $PM_{2.5}$ concentration over space and time. Our study draws a complete picture of the changes in $PM_{2.5}$ and its possible influences, which could guide future actions to mitigate $PM_{2.5}$ pollution in eastern China.

Keywords: fine particulate matter; spatiotemporal trend analysis; natural and socioeconomic factors

Citation: Wang, W.; He, Q.; Gao, K.; Zhang, M.; Yuan, Y. Spatiotemporal Trends and Influencing Factors of $PM_{2.5}$ Concentration in Eastern China from 2001 to 2018 Using Satellite-Derived High-Resolution Data. *Atmosphere* **2022**, *13*, 1352. https://doi.org/10.3390/atmos13091352

Academic Editor: Regina Duarte

Received: 29 June 2022
Accepted: 20 August 2022
Published: 24 August 2022

1. Introduction

Exposure to ambient fine particulate matter ($PM_{2.5}$) has been found to threaten the human body globally, triggering respiratory [1] and cardiovascular diseases [2] and even premature mortality [3,4]. According to [4], $PM_{2.5}$ ranked as the fifth leading fatal risk in 2015 and was responsible for 4.2 million premature mortalities worldwide. In order to fight this widespread environmental threat, a comprehensive understanding of the spatiotemporal variations of ambient $PM_{2.5}$ exposure and the possible influencing forces underlying $PM_{2.5}$ variations is essential for policymakers to make targeted strategies to regulate air quality and reduce the risks associated with $PM_{2.5}$ exposure.

As a side effect of fleeting economic development and industrialization, China has experienced severe air pollution in recent decades [5,6]. Particularly, eastern China, one of the most densely populated areas globally that possesses only a third of the Chinese territory, while accommodating more than 80% of the Chinese population, has suffered from heavy $PM_{2.5}$ pollution, attracting increasing concerns worldwide [7]. To remedy this issue, China has implemented successive measures and policies, thus working on mitigating anthropogenic emissions and preventing air pollution since 2006 [8,9], e.g., upgrading facilities in power plants to reduce SO_2 and NOx emissions [10]. Even stricter clean air actions have been imposed since 2013 to enact a new national air quality standard, and a national network was also established to monitor the air quality regularly [11].

Since these actions, the national $PM_{2.5}$ concentration has been decreasing significantly. However, the driving factors that led to these significant decreases are still unclear, and many factors could play a role since the $PM_{2.5}$ concentration has great spatiotemporal heterogeneity. On the one hand, a large number of local air pollutants contribute to forming a heavy haze in eastern China, with transboundary air pollution and unfavorable dispersion associated with the intricate terrain and climatological conditions exacerbating the pollution levels [12,13]. On the other hand, the national and regional clean air actions have modified the energy consumption structures and the spatial emission pattern, both of which would drive the spatiotemporal pattern of air quality to deviate from the original track [14,15]. Therefore, to further instruct future emission regulation strategies, it is crucial to update a detailed analysis of the $PM_{2.5}$ changes over space and time in eastern China and comprehensively understand the factors affecting $PM_{2.5}$ variation in this region.

By using ground-based $PM_{2.5}$ monitoring datasets, many studies have explored the spatial-temporal patterns of $PM_{2.5}$ pollution and its affecting factors in China [16–22]. While such ground-level measured $PM_{2.5}$ data have the advantage of high accuracy and high temporal resolution and can, therefore, accurately elucidate short-term variations, they are limited in their short observation period and capacity to explore the urban details of $PM_{2.5}$ changes because the monitoring sites are sparsely distributed and were only constructed in the past few years. By taking advantage of the global annual ambient $PM_{2.5}$ concentration datasets, estimated from satellite remote sensing from [6], an increasing number of studies have been dedicated to investigating the long-term characteristics of $PM_{2.5}$ pollution and its influencing factors for China at a finer spatial scale [7,23–26]. Despite the longer and wider study domains, such studies are limited in revealing the seasonal features of $PM_{2.5}$ exposure. In addition, most of the existing literature adopted simple methods, such as correlation analysis and linear regression models, to explore the underlying affecting mechanisms of $PM_{2.5}$ variations [7,16,20,23]. However, the linear models adopted cannot fully present the relationship between $PM_{2.5}$ and its influencing factors because they all highly vary in space over time. Thus, the complicated relationship between $PM_{2.5}$ and its influencing factors, with long-term trends and short-term variation characteristics at a fine spatial scale, remains to be uncovered.

Several previous studies have examined the impact of the natural factors that affect the formation and dispersion of $PM_{2.5}$, e.g., planetary boundary layer height, wind speed and direction, and temperature, in both the short-term variation and long-term trend of $PM_{2.5}$ [7,18,27,28]. In addition, an increasing number of studies have explored the relationship between $PM_{2.5}$ and socioeconomic factors, such as GDP per capita, traffic volume, and population, to identify the influence of the anthropogenic activities associated with economic development and industrialization on $PM_{2.5}$ exposure [26,29]. However, little is considered about how the strict emission control policies rolled out in recent years are related to the $PM_{2.5}$ changes, especially in eastern China, where the dense population results in intensive human activities. Moreover, there are few previous works that have simultaneously investigated the influence of both the natural and human aspects [24,30].

To fill the knowledge gap left by the existing literature, the main objective of this study is to employ long-term $PM_{2.5}$ data with high spatiotemporal resolution and advanced methods that allow us to explore the spatial and temporal heterogeneity in the data to present a complete picture of the changes in $PM_{2.5}$ and how the natural and human influencing factors are linked to these changes. We first plotted the spatiotemporal variations of the ambient $PM_{2.5}$ concentrations in densely populated eastern China at multiple spatial and temporal scales. Then, a piecewise linear trend analysis was used to explore the differences in the $PM_{2.5}$ changes for eight urban agglomerations. The impacts of both natural and human conditions on the long-term $PM_{2.5}$ trend and spatial disparities were identified using geographically weighted regression and a geographic detector model.

2. Materials and Methods

2.1. Study Region

The study domain covers eastern China, comprising 20 provinces located between 20.22° and 42.62° latitude and 101.92°and 122.95° longitude (Figure 1). With an entire extent of approximately 2,800,000 km^2 and a total population of about 1.05 billion residents in 2010, the East China region is one of the most densely populated regions worldwide and is confronting a severe $PM_{2.5}$ pollution issue [7]. Moreover, the eight populous urban agglomerations, including five national agglomerations (UA1-UA5 in Figure 1) and three regional agglomerations (UA6-UA8 in Figure 1), were also selected as regions of interest for the subsequently spatiotemporal trends and influencing analyses. Please note that western Sichuan was excluded from the present study because, with a relatively sparse population and lower $PM_{2.5}$ levels, its natural and anthropogenic environment differs from eastern Sichuan [31].

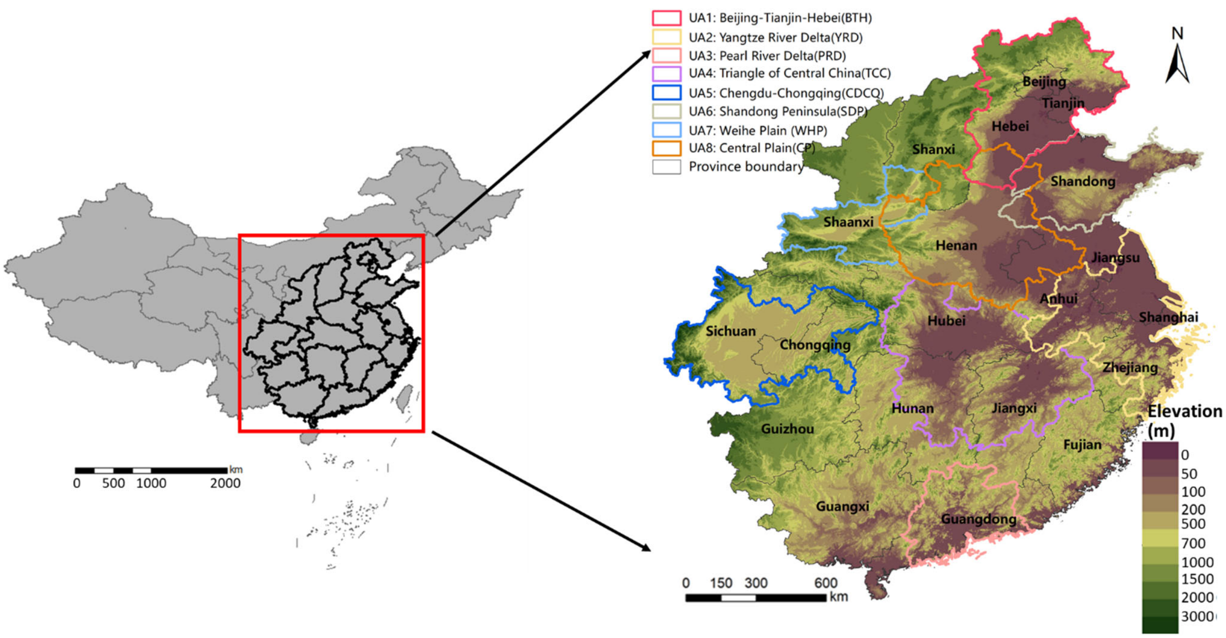

Figure 1. Study region of the present work, showing the eight urban agglomerations and terrain.

2.2. Data

2.2.1. Satellite-Derived $PM_{2.5}$ Predictions

We extracted the monthly and yearly average 1-km $PM_{2.5}$ predictions during 2001–2018 from our previous study [31]. The daily 1-km $PM_{2.5}$ estimates are publicly available via http://doi.org/10.5281/zenodo.4569557 accessed on 28 June 2022. The model development and validation were explicitly described elsewhere and briefly summarized in this study. It is challenging to estimate the ground-level $PM_{2.5}$ over China before 2013 because the $PM_{2.5}$ measurements used as the dependent variable in the statistical modeling were not recorded in those historical years. To predict daily $PM_{2.5}$ before 2013, we employed an adaptive modeling framework, relying on a seasonal GTWR (geographically and temporally weighted regression) that can effectively capitalize on local spatiotemporal information. The seasonal GTWR model was improved from the popular GTWR model [32] by considering the seasonality in the weighing matrix. The satellite-derived high-resolution aerosol product, i.e., the Multi-Angle Implementation of Atmospheric Correction (MAIAC) 1-km AOD dataset; the meteorological parameters, including the planetary boundary layer height, relative humidity, temperature, wind speed, and pressure; and the land use-related variables, including the Normalized Difference Vegetation Index (NDVI) and elevation, were employed in the spatiotemporal modeling. Both the linear terms and non-linear interaction between the AOD and meteorological variables were used to help the model capture the spatiotemporal variability of the data. A rigorous evaluation method, i.e., the leave-one-year-out cross-validation method, was adopted to evaluate the historical estimates. In addition, an offset validation against the measurements from the U.S. embassies was conducted to verify the model's performance outside the modeling years. Those validation results show that the nationwide predictions achieve a good agreement with ground-level measurements, especially at monthly and yearly timescales. Here, we compared the monthly and yearly 1-km $PM_{2.5}$ predictions over eastern China with the ground-level $PM_{2.5}$ observations. As shown in Figure A1, the monthly and yearly average $PM_{2.5}$ concentrations precisely accounted for the 73% and 79% variations in the corresponding $PM_{2.5}$ values, indicating that the subset of the historical estimates can be used to investigate the spatiotemporal variation and influencing factors analysis of $PM_{2.5}$ in eastern China in 2001–2018.

2.2.2. The Influencing Factor Data

Both natural and anthropogenic factors were used to identify the impacts of $PM_{2.5}$ change. The five socioeconomic indicators were collected from the *China City Statistical Yearbook of 2002 to 2019*, including (1) the GDP per capita, measuring the regional economic growth; (2) population density, indicating the intensity of anthropogenic activity; (3) the size of the built-up area, reflecting the level of urban development; (4) the proportion of industry to GDP as a proxy of the industrial structure and emission; (5) road area, representing traffic intensity. The socioeconomic indicators were the annual data at the city level. The definitions and data sources for these factors are detailed in Table 1.

The natural factors are the four main meteorological variables: relative humidity, temperature, wind speed, and planetary boundary height, which were the station monitoring data obtained from the China Meteorological Science Data Center. To spatiotemporally match the socioeconomic data, the annual average values for each city were calculated.

Table 1. Data sources for influencing factors used for influencing factor analysis.

Variables	Definitions	Units	Data Sources
Relative humidity	Relative humidity	%	China Meteorological Science Data Center
Temperature	Temperature	°C	China Meteorological Science Data Center
Wind speed	Wind Speed Rate	m/s	China Meteorological Science Data Center
Boundary layer height	Planetary boundary layer height	m	China Meteorological Science Data Center
Built-up area	Built-up area	km^2	China city statistical yearbook
Population_density	Population density	persons/km^2	China city statistical yearbook
GDP_per_capita	Per Capita GRP (Gross Regional Product)	Chinese yuan	China city statistical yearbook
Industry_ratio	Secondary Industry as Percentage to GRP	%	China city statistical yearbook
Road_area	Area of City Paved Roads at Year-end	$10^4 m^2$	China city statistical yearbook

2.3. Statistical Analysis Methods

2.3.1. Trend Analysis of $PM_{2.5}$ Variation

Both regional- and pixel-based trend analyses were conducted in this study. Since the regional/national long-term $PM_{2.5}$ trend does not change monotonously [9,33,34], a piecewise linear regression technique, based on a Bayesian approach, was used to thoroughly explore the long-term trend, which captures the turning character of 18-year trends according to the monthly population-weighted mean $PM_{2.5}$ anomaly time series. Similar piecewise linear trend analyses were also conducted in previous studies to investigate a better $PM_{2.5}$ variation in the long run [25,35]. The critical task for a piecewise linear trend model is to identify the appropriate turning point(s) at which data changes substantially. According to previous studies [35] and the monthly time series shown in Figure A2, three pieces, i.e., two turning points, may appropriately describe the changing trend. The R^2 and RMSE were calculated in Table A1 in the context of having no inflection point (one-piecewise line), one inflection point (two-piecewise line), and two inflection points (three-piecewise line), which presents that in most cases, the three changing pieces are better compared with those having no inflection point or one inflection point. Of course, the time series can be partitioned into four or more pieces; however, the more inflection points, the shorter the period for each time series piece. As we aimed to thoroughly explore the long-term trend and examine the effectiveness of the emission control policies explicitly, separating the time series data into too many pieces is pointless. Moreover, a simpler model is more favored than a more complicated one because it is easier to implement and test [36,37]. Thus, the three pieces with two turning points were used in this study.

The piecewise linear trend estimate was implemented in MATLAB R2017b and based on a Bayesian approach (John D'Errico 2021; https://www.mathworks.com/matlabcentral/fileexchange/24443-slm-shape-language-modeling (accessed on 28 June 2022)).

In addition, a pixel-based general least square (GLS) regression (see details in [38]) was conducted to detect the long sequential $PM_{2.5}$ change. To minimize the seasonal effect within the data, we applied monthly mean $PM_{2.5}$ anomalies to the GLS regression, calculated by subtracting the climatological monthly mean. Such a linear trend method has been widely used in environmental analyses [11,39]. A locally weighted linear regression (LOWESS) technique was used to smooth the gridded $PM_{2.5}$ because the highly spatiotemporally varying $PM_{2.5}$ caused many $PM_{2.5}$ pixels to be statistically insignificant.

2.3.2. Quantitative Analysis of Influencing Factors on $PM_{2.5}$ Variation

To explore the characteristics of the natural and socioeconomic factors on the $PM_{2.5}$ concentration, we employed two advanced statistical techniques, i.e., the geographically weighted regression (GWR) [40] model and the geographical detector model [41]. Through a spatial distance-based weighting matrix, the GWR model can handle the spatial variability within the data and estimate a spatial continuous surface of coefficients for each local regression. These estimated coefficients can be used to identify the space-varying feature in the relationship between $PM_{2.5}$ and the latent influencing factors. This study used a city-level mean $PM_{2.5}$ as the response variable and influencing factors as the independent inputs. The variables and data sources used for the impact factor analysis are described in Section 2.2.2. To ensure comparability, standardized coefficients of slopes were used to assist the determination.

The geographical detector model was employed for the influencing factor analysis, which has been increasingly used in studies on socioeconomic factors of environmental risks [17,26]. The details of this technique have been summarized in [41] and will only be briefed here. By not relying on a linear hypothesis in the linear regression models, geodetector holds the potential to discover the impact factors underlying spatial stratified heterogeneity, as determined by comparing the difference in the variances of the factors between sub-regions and an entire area. The fundamental principle is that if an influencing factor (e.g., GDP) possesses a spatial pattern similar to the risk (e.g., $PM_{2.5}$ level in this study), this factor affects the risk to a certain degree. The Q-statistic is used to identify the power of the influencing factor. Usually, q is between 0 and 1, and the larger the q value is, the greater influence the factor has on the risk.

The multiple linear regression (MLR) model was also used for the impact factor analysis. The slope of the MLR model can indicate the angle and the average speed of the acceleration of the prevailing linear regression trend between ground $PM_{2.5}$ and the selected factor. That is, the positive and negative slopes represent the positive and negative correlations between $PM_{2.5}$ and the selected factor, respectively, and the larger the absolute value of the slope is, the steeper the regression line and the greater the rate of the change is. To identify the collinearity issue between the ground $PM_{2.5}$ and the nine factors, an MLR model with collinearity analysis was preliminarily performed on the multi-year mean values. The collinearity statistics are documented in Table A2, with variance inflation factor values less than 10 and a tolerance greater than 0.1, which demonstrates a slight collinearity problem in the data.

We implemented the GWR model and geo-detector analysis in ArcGIS 10.0 and the software provided by [41]. All the other spatiotemporal analyses were conducted in MATLAB R2017.

3. Results and Discussion

3.1. Spatiotemporal Pattern of Predicted $PM_{2.5}$

Figure 2 shows the spatiotemporal variations of the ground-level $PM_{2.5}$ concentrations from 2001 to 2018. In general, due to intensive anthropogenic activities, long-transported dust, and unfavorable dispersion terrain, greater than 70% of the study area, equivalently more than 80% of the Chinese population, has been suffering from risky $PM_{2.5}$ concentrations during the eighteen study years, which are higher than the national secondary level limit of 35 μg/m^3. The year-to-year $PM_{2.5}$ data also demonstrated that the annual patterns of $PM_{2.5}$ are similar to each other and in line with the multi-year mean distribution, corresponding to previous studies [31,42]. Spatially, southern Hebei was the most $PM_{2.5}$-polluted area, with most $PM_{2.5}$ levels being >75 μg/m^3. Other severely $PM_{2.5}$-polluted regions included the North China Plain (NCP), the Chengdu-Chongqing (CDCQ) region, Weihe Plain (WHP, UA7 in Figure 1), and the eastern Hunan-Hubei region, where most of the residents were usually living under dangerous $PM_{2.5}$ levels (>55 μg/m^3). In eastern China, a few areas demonstrated $PM_{2.5}$ as satisfying the annual 35 μg/m^3 standard and were primarily located in regions with relatively less population, such as northwestern Hebei, western Hunan, Fujian, and southern Zhejiang. Figure A3 demonstrates that the seasonal patterns generally mirror each other and the spatial variation of the multi-year mean $PM_{2.5}$ but notably varies in pollution levels. Winter was the most polluted season, with the largest mean (64.37 μg/m^3) and coefficient of variation (CV, 0.38) values. Although summer has the smallest average value, $PM_{2.5}$ pollution in this season is also worthy of attention because of its significant spatial contrast (CV = 0.38).

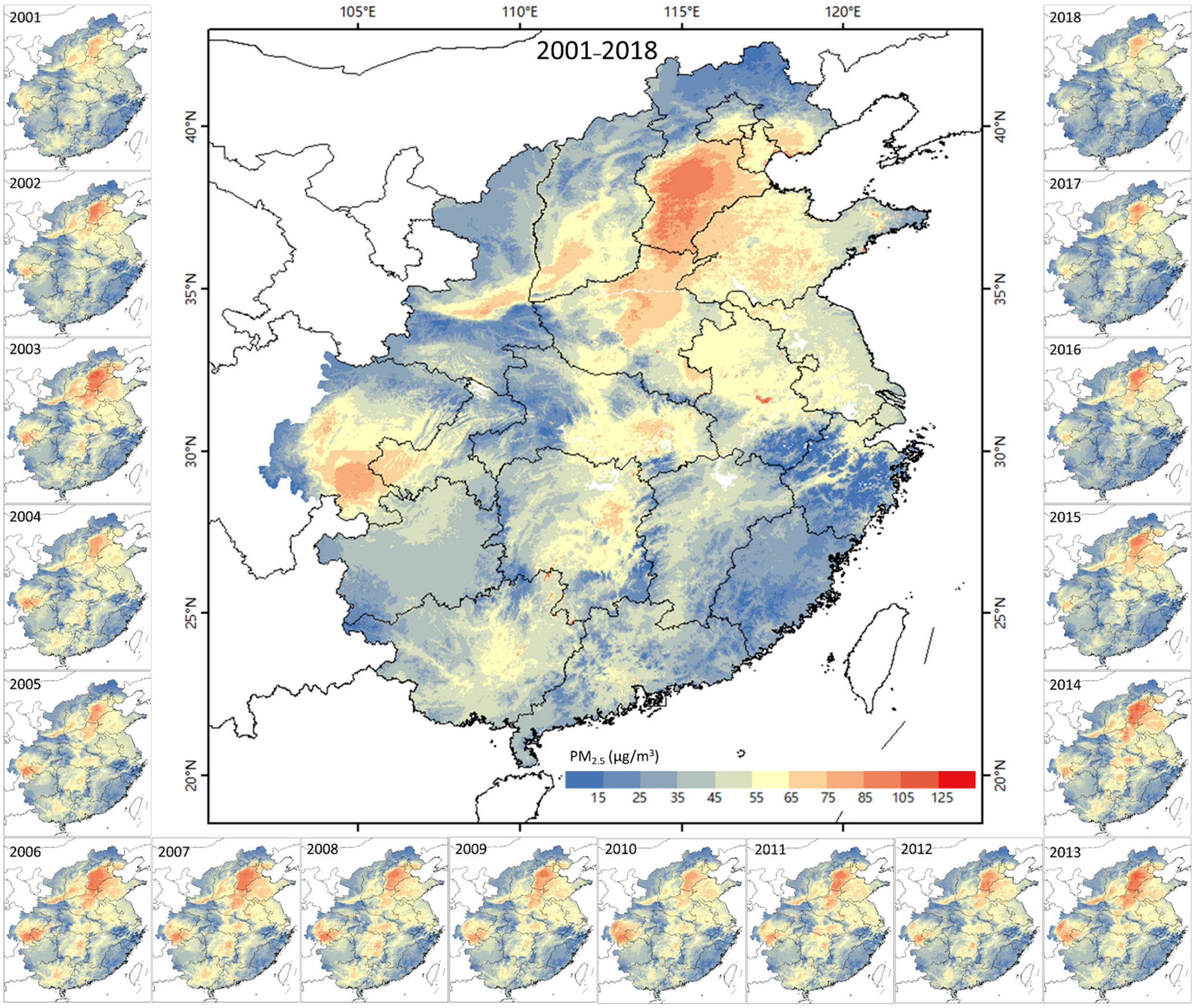

Figure 2. Spatial maps of 1-km $PM_{2.5}$ concentrations over eastern China in 2001–2018.

We also looked at the spatiotemporal changes in $PM_{2.5}$ in the populous urban agglomerations during 2001–2018 (Figure 2). Among the eight agglomerations (Figure 1), the Central Plain (CP) and Shandong Peninsula (SDP) regions were the most polluted, followed by the Beijing-Tianjin-Hebei (BTH) and CDCQ regions, and the Pearl River Delta (PRD) area was the cleanest, where the regional multi-year $PM_{2.5}$ averages during the eighteen years were 59.77 μg/m^3, 59.16 μg/m^3, 52.27 μg/m^3, 49.98 μg/m^3, and 40.98 μg/m^3, respectively. However, when overlaying the $PM_{2.5}$ distribution with the population map, the situation was different (Figure A4). The long-term exposure to $PM_{2.5}$ reached its maximum over the BTH region, whose population-weighted mean $PM_{2.5}$ concentration was 69.02 μg/m^3, which greatly exceeded the study-area mean value (54.98 μg/m^3). The PRD region maintained the lowest value in terms of exposure, with a population-weighted mean $PM_{2.5}$ of 46.85 μg/m^3.

Figure 3 shows the spatial distribution of the $PM_{2.5}$ trends over eastern China from 2001–2018. Broadly, the $PM_{2.5}$ concentrations in the majority of the study region demonstrate downward tendencies in the past 18 years. Specifically, evident decreasing tendencies with a slope of <−0.25 μg/m^3/yr ($p < 0.05$) were widespread in the southern areas, including most of the CDCQ region and were extensive in the adjacent areas of the Guangxi, Hunan, Jiangxi, and Guangdong provinces. However, the spatial pattern of the $PM_{2.5}$ trends in the northern provinces was complex. Weak negative trends, with slopes between

−0.25 μg/m³/yr and 0, dominated in the north of the study region, and stronger slopes (<−0.25 μg/m³/yr) were only scattered over the inland provinces. It should be pointed out that statistically significant positive trends ($p < 0.05$) were observed in considerable areas of the northern provinces; among those upward trends, pronounced increasing slopes (>0.1) occurred primarily in the coastal areas (e.g., Shandong peninsula and Jiangsu). There were still many increasing trend areas occurring under the intense air pollution control policies, indicating that the ongoing policies should continue and even be stricter. Despite the various levels of trends, the adjacent areas generally show similar directions and statistical significance in the long-term $PM_{2.5}$ change (Figure 3), suggesting that cities/regions need to coordinate their goals between economic development and air pollution improvement and take joint actions to alleviate $PM_{2.5}$ pollution, which may amplify the measures and policies.

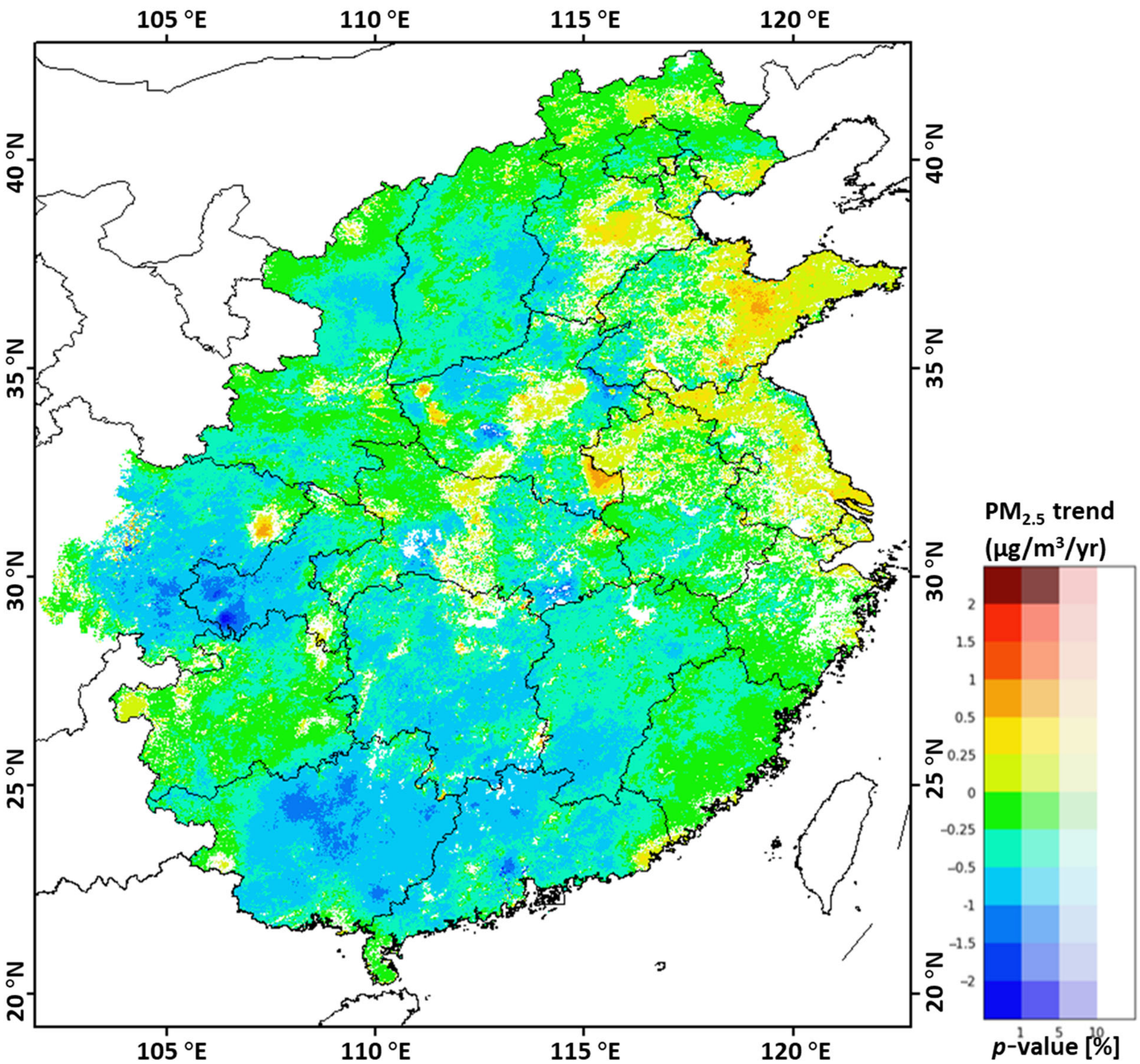

Figure 3. Spatial map of estimated GLS trends based on LOWESS-smoothed monthly time series $PM_{2.5}$ from 2001 to 2018. The color of the grid cell represents the slope of the trend, and the transparency of colors stands for the statistical significance level of the trend.

Figure A5 presents the spatial map of the linear trends in satellite-derived $PM_{2.5}$ concentrations for each specific season, indicating a potent seasonal dependence on the downward trends over the study region. The largest yearly decreasing trends, at the statistical significance of a 95% confidence level, were predominantly observed in winter, at an average rate of up to −0.96 μg/m^3/yr, followed by autumn (−0.67 μg/m^3/yr). Summer and spring exhibited a slower decrease, with a mean of −0.33 μg/m^3/yr and −0.24 μg/m^3/yr, respectively. Similar to the spatial heterogeneity feature shown by the seasonal $PM_{2.5}$ concentration, the change in seasonal $PM_{2.5}$ levels also presented significant spatial variabilities. Such apparent spatial and seasonal variabilities in $PM_{2.5}$ trends imply that the seasonal impact of the various natural factors (e.g., meteorological contributors) on air quality could not be ignored. Thus, when making an air quality policy and evaluating the effectiveness of the relevant policies, the effects on the $PM_{2.5}$ variation caused by seasonal factors should not be counted because those policies are inclined to impose controls/restrictions on anthropogenic activities.

On the one hand, China has undergone rapid urbanization and industrialization over the past two decades, emitting substantial pollutants into the atmosphere. On the other hand, a series of air quality control policies have been promoted to reduce anthropogenic emissions significantly. Consequently, the joint effect results in a non-monotonously change in $PM_{2.5}$ over time. The heterogeneity illustrated by the time series of coefficients of variation in eastern China (Figure A2) also shows an increasing trend with the inflection feature. Thus, we further conducted a Bayesian-based piecewise linear trend technique (see the details in Section 2.3.1) to detect the turning points for the temporal trend in $PM_{2.5}$. The modeling uncertainty results are summarized in Table A1. In general, three pieces with two turning points were used to profile the long-term changing trend for each agglomeration. However, we used two pieces to describe the long-term trend for Weihe Plain and Central Plain, although the three-piece models performed better because we found that a turning point almost overlaps the start-/end-point in the three-piece model.

Figure 4 plots the monthly time series of the population-weighted mean $PM_{2.5}$ anomalies for eastern China and eight megacity regions, with corresponding piecewise linear trends. The monthly time series averages for the entire domain exhibit a decreasing trend, with a slope of −0.23 μg/m^3/yr from 2001 to 2018, which resulted from the offset of positive and negative trends across eastern China over the long term, as shown in Figure 3. The population exposure to $PM_{2.5}$ over entire eastern China was divided into three stages, and two inflection years were derived, 2007 and 2014. Due to the rocketing economic growth and loose emission policies, a marked increase was observed in the first 2001–2006 stage, at a rate of 1.14 μg/m^3/yr. Driven by the tightened emission and energy policies implemented since 2006 [8,9], such as the use of desulfurized facilities in the industry and the closure of severely polluting manufactories due to the 2008 Beijing Olympic Games, the medium 2007–2013 stage switched to a weak decreasing trend with a slope of −0.17μg/m^3/yr. In the later stage, the regional trend changed notably, and an extreme decreasing tendency (slope= −2.25 μg/m^3/yr) occurred as a consequence of more stringent emission control and air pollution prevention policies, such as the Action Plan of Air Pollution Prevention and Control from 2013 onwards. The spatial distributions of Figure A6 decompose the overall trends for the three stages, showing that the inconspicuous regional trend within the medium stage was a synthetic result of larger increasing trends, predominantly in the north, and significant decreasing trends prevailing in the south. Moreover, the implementation of mitigation measures and policies did not lead to an immediate consequence because both regional trend transitions were one-to-two years behind policy implementation.

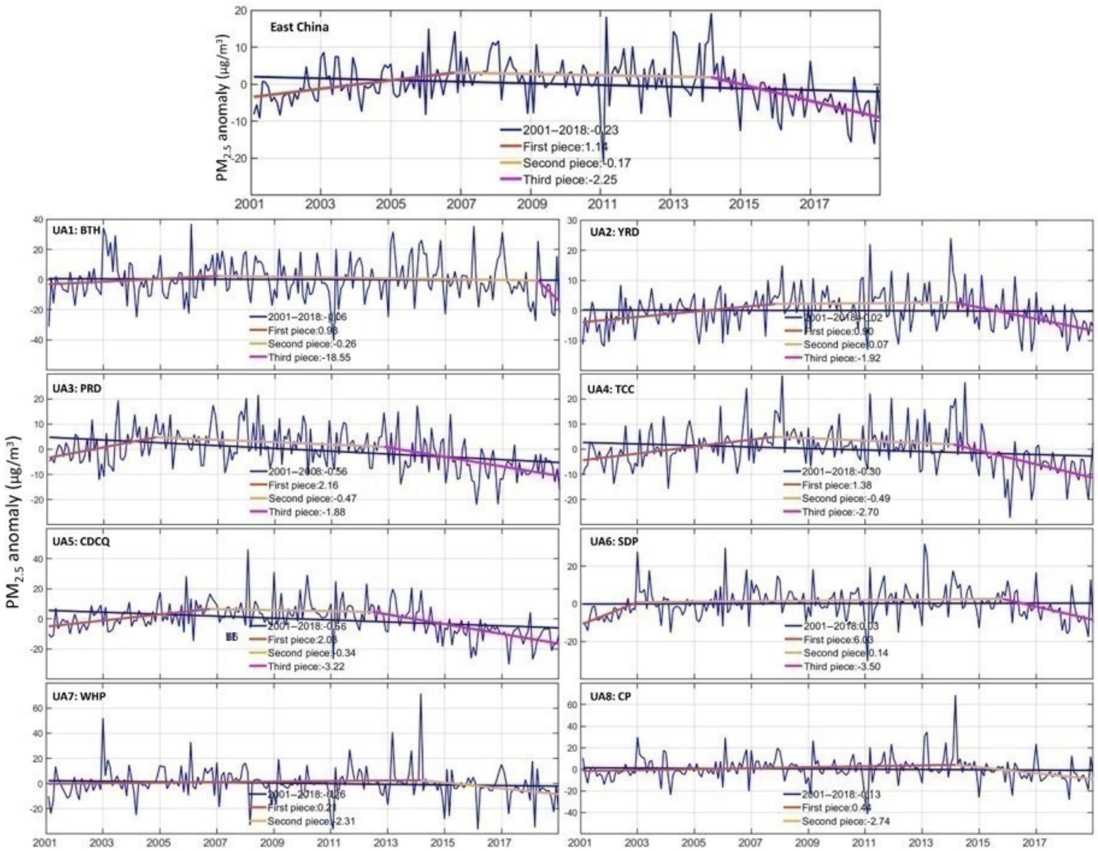

Figure 4. Monthly time series of population-weighted mean $PM_{2.5}$ predictions from 2001 to 2018 in the entire study region and eight urban agglomerations with corresponding piecewise linear trends. The grid population data were from [43].

Corresponding to the overall temporal pattern in eastern China and the previous studies [33,34], a similar inverse U-shape trend was observed in most megacity regions; however, the local trend's transition features also arose (Figure 4). Over the five national urban agglomerations, the first local turning year occurred predominately between 2005 and 2008, accompanied by a distinct increasing trend, varying between 0.90 μg/m³/yr and 2.16 μg/m³/yr in the first stage; the second trend's transition appeared mainly between posterior 2013 and 2016, possessing a noticeable decreasing tendency (−1.88~−3.22 μg/m³/yr), except for BTH, which experienced the second inflection year until 2018 with a slumping slope of −18.50 μg/m³/yr. As for the regional agglomerations, the SDP region, where the first local transition year was before 2003, underwent the second breaking point after 2016. All six agglomerations experienced a plateau between the two turning points, with a mild local slope of −0.49~0.14 μg/m³/yr. According to our piecewise linear model fitting results (Table A1), the two regional agglomerations, the WHP and CP regions, did not possess the general U-shape trend, while the two-piece trend with one turning point can better interpret the local trend's transition. $PM_{2.5}$ exposure in the two agglomerations started to decline in 2014 after experiencing a long-term slow elevation, showing a positive slope of 0.21 μg/m³/yr for WHP and 0.44 μg/m³/yr for CP, respectively. These findings suggest that in addition to the country's air quality policies, the local policies, and measures tailored for the regional economic and atmospheric condition, e.g., altering the production structure, adopting clean energy, and adjusting the intensity of emission reduction, should also be enacted and actualized to guarantee the country's goal of air quality improvement.

3.2. Factors Affecting Changes in $PM_{2.5}$

As illustrated in the previous sections, the regional $PM_{2.5}$ pattern was markedly influenced by many natural and anthropogenic factors. To examine the factors influencing the $PM_{2.5}$ concentration, we deployed the GWR model and geographical detector in this section. Paying heed to the results from previous studies [12,17,26,29,30] and giving consideration to the availability of city-level data, we quantitatively examined the influence of four meteorological factors and five socioeconomic factors. The definitions and data sources for these factors are detailed in Table 1. Figure 5 shows the standardized coefficients of slopes from multiple linear regressions and the power of determinant values (q) from the geographical detector from 2001 to 2018. In general, the four selected natural factors, with a larger averaged q value (0.18), imposed more significant impacts than the five selected socioeconomic factors (0.12); however, each of these nine factors has its own characteristics.

Among the four meteorological factors, temperature, with the largest mean q value of 0.28 in the 18 study years, made the predominant contribution to the spatial variability of $PM_{2.5}$ concentrations, according to the geographical detector results (Figure 5a). However, the results generated from the multiple linear regression (MLR) model (Figure 5b) demonstrate that the temperature was insignificantly correlated to $PM_{2.5}$ throughout the study's time span, except in 2016 and 2018. The contrasting outcomes may result from the difference between the two techniques. In general, ambient temperature interacts with atmospheric aerosols in a complicated way [44], such that a linear model like MLR is insufficient to describe the nonlinear relationship. It further corroborates that the nonlinear predictors used in the $PM_{2.5}$ estimation positively impact the model's accuracy [31]. The geographical detector recognizes the crucial impacts of the changes in relative humidity associated with the ubiquitous hygroscopic growth of aerosols and boundary layer height related to the particle dispersion on fine ambient particles, with mean q values of 0.22 and 0.13, respectively. Over a small-scale area in a short-term period, ambient concentrations of $PM_{2.5}$ can be significantly affected by wind speed, but the situation may be complicated over a large-scale region in a long-term interval. At the yearly timescale, wind speed proved to have a weak effect on the $PM_{2.5}$ changes in eastern China (mean q value = 0.09 in Figure 5a).

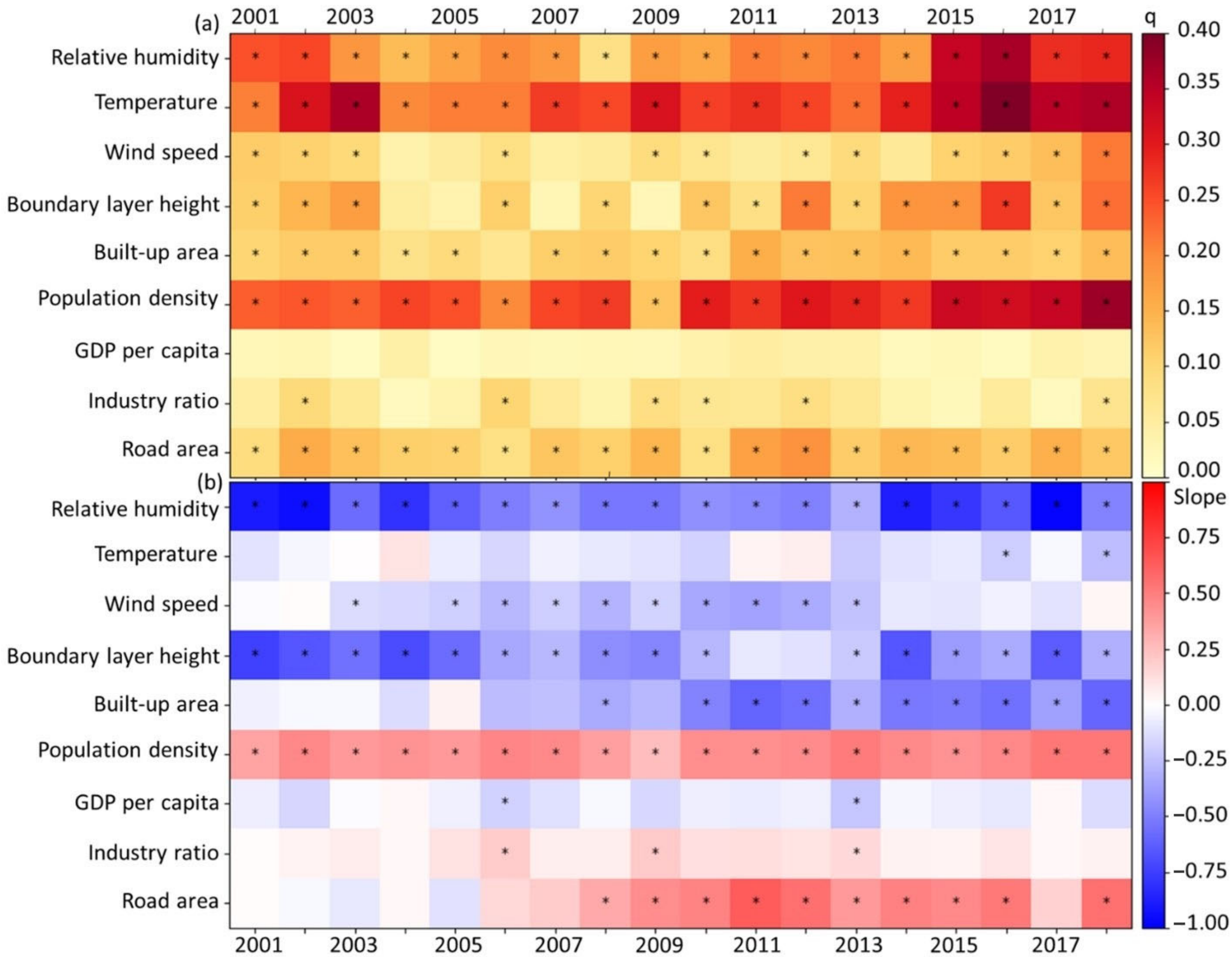

Figure 5. (**a**) Power of determinant value q and (**b**) standardized slope of a linear model for each impact factor from 2001 to 2018 in eastern China. Asterisk (*) in a square indicates it is statistically significant at a *p*-value of 0.05.

Population density (mean q = 0.27), compared to the other anthropogenic contributors, held the leading influence on the uneven distribution of $PM_{2.5}$ concentrations. A city with a denser population means that intensive anthropogenic activities are associated with air pollutant emissions and increased non-renewable energy consumption, which are understood to be principal sources of primary and secondary fine particles [45]. Thus, urban population density is believed to be one core factor for adjusting $PM_{2.5}$ pollution within cities. This result is also borne out by the larger standardized slope coefficients of MLR, indicating that population density has a stronger positive correlation with $PM_{2.5}$ concentrations (Figure 5b). With a mean q value of 0.13 and positive linear slopes, the road area imposes a solid positive force on $PM_{2.5}$ increases. Because road area is usually associated with traffic volume and vehicle emissions, the increasing traffic exerts an apparent inhibitory effect on $PM_{2.5}$ improvement. Similarly, the ratio of secondary industry exerted a strong influence on aggravating the $PM_{2.5}$ concentrations. In line with previous studies [16,17], we also found a weak negative correlation between $PM_{2.5}$ and GDP per capita, which may indicate that the more flourishing the city's economy is, the more awareness of environmental health there is [17,46]. Note that both the geo-detector and MLR results concerning GDP per capita are not statistically significant.

To discriminate the temporal characteristics of influence exerted by the factors on $PM_{2.5}$ variation in eastern China, we painted the year-to-year power of determinant values (q) in Figure 5. Combining Figures 5 and 6, the time-varying patterns based on these contributors can be explicitly identified. Unlike meteorological factors, which maintain an increasing influence on affecting $PM_{2.5}$ and vary over time (Figure 6a–d), the impact of the socioeconomic factors tends to be intricate and complex, with various tendencies. The built-up area is found to possess a successive increase in the positive influence on $PM_{2.5}$ mitigation over the study period, with the q value rising to 0.14 in 2018 from 0.10 in 2001 and the slope correspondingly declining to −0.60 from −0.03. The uptrend of the built-up area may be attributed to urban development in eastern China. A developed city is generally associated with an optimized demographic pattern and urban form. For example, an increased ratio of urban green space from 2001 to 2018 (Figure A7) resulted in an enhanced city's function in digesting air pollutants [29]. It thus implies that the more developed the urban city is, the greater the capacity it has to regulate air quality. This result may also support the argument mentioned in the last paragraph, i.e., that a prosperous economy gives rise to public awareness of environmental health.

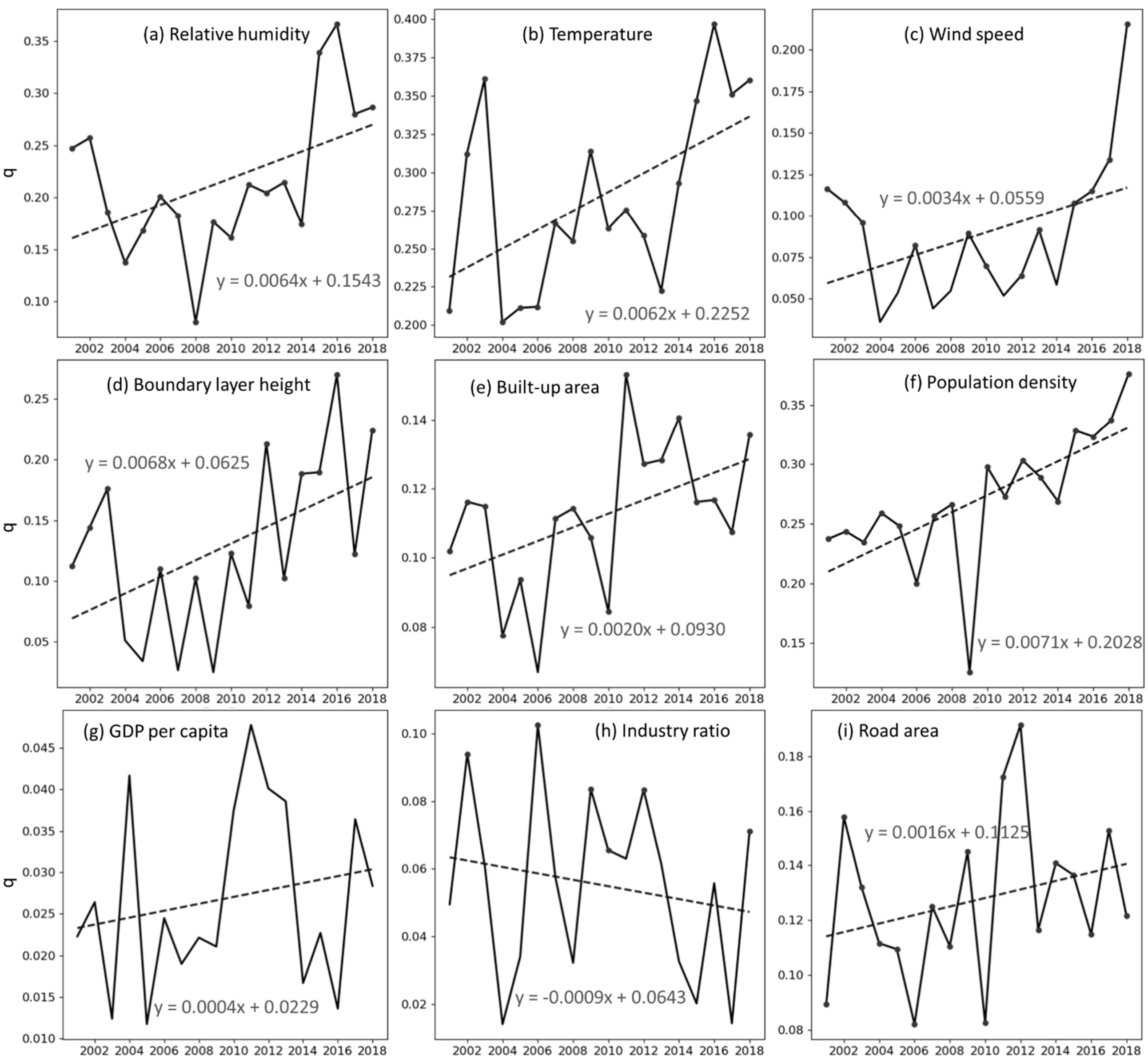

Figure 6. Scatterplots of power of determinant values (q) with their linear trend lines (dashed line) for each influencing factor from 2001 to 2018. The dot indicates a *p*-value below 0.05.

In contrast, we found that transportation exerted a more potent negative effect on $PM_{2.5}$ reduction, with a slight increase from 0.09 in 2001 to 0.12 in 2018, with statistically significant positive slopes for the road area variable in the later 18 years. With the growing economy and improved life quality, an increasing number of private vehicles are put into use, which relates to an incredible amount of automobile exhaust emissions. Consequently, the gradually enhanced role of the transportation factor in deteriorating air quality cannot be undervalued, particularly in recent years, and further stands as a severe issue for the future.

Interestingly, the secondary industry share shows a reduced contribution to affecting the changes in air pollutants throughout the study period, with a decreasing rate of −0.0009 in the power of the determinant value (Figure 6h). Such a decreasing trend was mainly attributed to the declining influence after 2012. Unlike the other socioeconomic factors that continuously impose an increasing impact on $PM_{2.5}$ in the whole study period, the ratio of the secondary industry shows an inflection point around 2012, before which an upward trend (slope = 0.0008) was observed. The stronger influence on $PM_{2.5}$ levels before 2013 was due to relatively loose emission policies with the fast industrialization in China, while the weakened influence of the industry sector on $PM_{2.5}$ concentrations after 2013 seems to be a consequence of implementing emission control measures and upgrading the industry structure. However, the outcome is likely not evident because the strength (slope = −0.0039 in recent years) was very small, and many q values were not statistically significant.

More interestingly, a closer inspection in Figures 5 and 6 indicates that the geo-detector q values of the built-up area, GDP per capita, industry ratio, and road area all possess obvious turning points around 2012–2013 and start to decline after years of ascension. Coincidentally, the city's mean $PM_{2.5}$ concentration began to decrease remarkably one or two years later (details are shown in Section 3.1). These findings imply that the air pollution improvement strategies, such as stricter clean air actions since 2013, may have caused the influences from the socioeconomic factors examined in the present work to be less effective. On the other hand, these results concerning potential anthropogenic factors of $PM_{2.5}$ variation also suggest that the air quality regulation strategies implemented in previous years have worked on $PM_{2.5}$ pollution alleviation to various degrees, so that future policies may be modified accordingly.

The GWR model was performed on the averaged data from 2001 to 2018, and Figure 7 visualizes the coefficient surfaces of the nine factors estimated by the GWR model. The adjusted R^2 value of the GWR model is 0.81, indicating that the resulting coefficients by GWR are appropriate for revealing the geographical discrepancies in the connection between $PM_{2.5}$ and its potential influencing factors. In general, the population density, road area, and industry ratio had prevailing positive correlations with $PM_{2.5}$ in most cities; the built-up area was dominated by negative correlations, and the other factors show evident contrasts in the correlations.

Figure 7 also demonstrates the significant spatial differences of the factors influencing the $PM_{2.5}$ distribution in eastern China. The strong positive temperature coefficients (standardized slopes > 5) were primarily observed in the northwestern cities, while they were all found to be negative in southeastern cities. The clear contrast in the temperature's connection with $PM_{2.5}$ between the southeastern and northwestern cities partially explains the large q value provided by the geo-detector model but statistical insignificance by the MLR model. Relative humidity and a built-up area were found to impose a strong inhibitory effect on the $PM_{2.5}$ aggravation in most regions. Boundary layer height sustained a negative association with the $PM_{2.5}$ variation in most southeastern and northwestern cities, but the intensity was weaker than temperature and humidity. The GWR model also shows a low correlation between the $PM_{2.5}$ distribution and GDP per capita, with standardized slopes between −1 and 1 in half of the cities. Broadly, the evident positive relationships between $PM_{2.5}$ and the population density, road area, and industry ratio were observed in most cities in eastern China, highlighting the extensive environmental pressures on urban cities exerted by increasing human activities. Overall, the significantly varying slopes from city to city indicate that distinct spatial disparities are widespread in the interactions between fine particles and their natural and human impact factors, which can partially account for the confusing results between the geographical detector model and the MLR model. More importantly, the marked spatial variability in the city-level $PM_{2.5}$-determinant relationship, revealed by the spatial model, suggests that the cities in the study area are significantly challenged by different air pollution problems, and targeted $PM_{2.5}$ mitigation regulations, therefore, need to be promulgated according to the city's distinct natural and anthropogenic conditions.

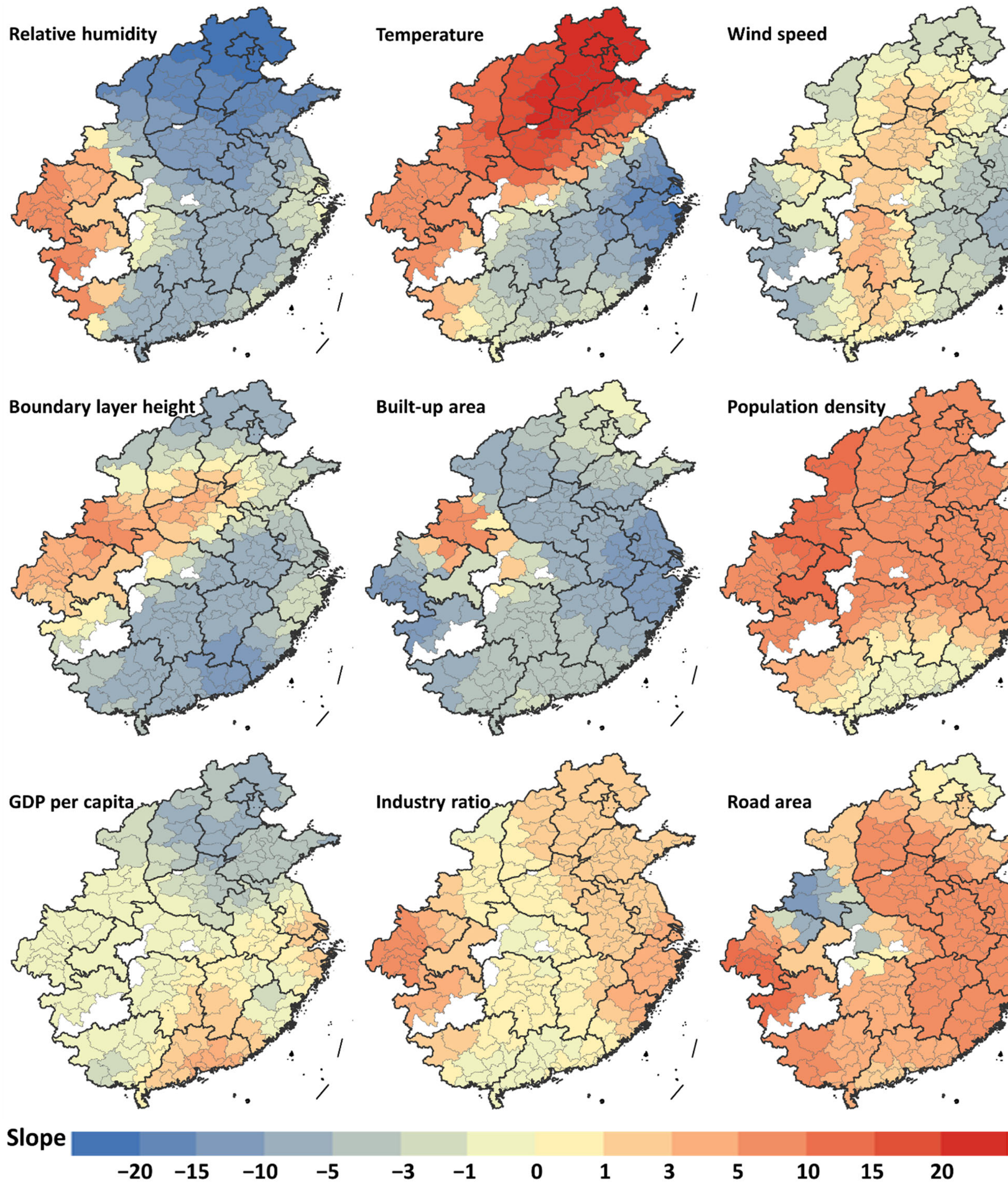

Figure 7. The space-varying coefficients of GWR models for each influencing factor based on the average data from 2001 to 2018.

4. Conclusions

Space and time are fundamental when considering the $PM_{2.5}$ variations, and so are its possible influencing factors. Upon the high-resolution $PM_{2.5}$ estimates in a long-term period, we explicitly describe the spatiotemporal pattern of the population to $PM_{2.5}$ for the study domain at multiple spatial and temporal scales. Long-term $PM_{2.5}$ predictions show that most of eastern China suffered from risky $PM_{2.5}$ exposure, particularly in densely populated urban agglomerations, such as the BTH region. We find that the regional $PM_{2.5}$

levels experienced an inverse-U shape trend, and the two turning points were around 2007 and 2014. Most of the discernable decreasing trends occurred in the southern and western areas of the study domain, and almost no statistically significant trends and increasing trends were primarily in the NCP region. In the last four or five years, the local air quality has improved vastly, which benefited predominantly from a series of efforts on mitigating emission policies and clean air measures.

On the basis of the geo-detector, GWR model, and MLR model, the influencing factors of $PM_{2.5}$ were quantitatively examined, offering consideration to the spatial disparities and temporal differences. In general, relative humidity, temperature, wind speed, boundary layer height, built-up areas, population density, industry ratio, and road area made statistically significant contributions to ground-$PM_{2.5}$ variance, among which temperature and population density exerted more potent effects than the other influencing factors. The trend analysis and GWR results present the spatiotemporal heterogeneity in the connections between $PM_{2.5}$ and the factors: temporally, all the natural and socioeconomic variances exhibited ever-increasing contributions to $PM_{2.5}$, with the exception of the industry ratio, which showed a slightly decreasing trend; spatially, population density, road area, and industry ratio possessed prevailing positive correlations with $PM_{2.5}$, the built-up area was dominated by negative relationships, and the other factors showed evident contrasts in the correlations in most cities in eastern China.

Though the findings of this study enrich the long-term $PM_{2.5}$ changes and correlations with the influencing factors, this study has some limitations that can be further examined in the future. First, the uncertainty in the $PM_{2.5}$ estimates may bias the monthly and annual averages of $PM_{2.5}$ and further bias the trend and influencing factor analyses. Further improvement in $PM_{2.5}$ estimations is needed. Second, we only selected four natural and five anthropogenic factors to conduct the influencing factor analysis and such a factor analysis was performed on a city level due to the lack of appropriate data. More socioeconomic data and sources of emissions associated with $PM_{2.5}$ can be attempted in future studies.

Author Contributions: Conceptualization, Q.H.; methodology, Q.H.; formal analysis, W.W. and K.G.; resources, Q.H.; data curation, W.W.; writing—original draft preparation, W.W. and Q.H.; writing—review and editing, W.W., Q.H., M.Z. and Y.Y.; visualization, W.W. and K.G.; supervision, Q.H. and M.Z.; funding acquisition, Q.H. and Y.Y. All authors have read and agreed to the published version of the manuscript.

Funding: This research was funded by the National Natural Science Foundation of China (Grant NO. 41901324 and 52079101).

Institutional Review Board Statement: Not applicable.

Informed Consent Statement: Not applicable.

Data Availability Statement: The daily 1-km $PM_{2.5}$ estimates are publicly available via http://doi.org/10.5281/zenodo.4569557 accessed on 28 June 2022.

Conflicts of Interest: The authors declare no conflict of interest.

Appendix A

Table A1. The calculated R^2 and RMSE for the monthly population-weighted mean $PM_{2.5}$ time series in the study region and eight urban agglomerations under the conditions with no turning point, one turning point and two turning points.

Study Area	No TP		One TP			Two TPs			
	R^2	RMSE	R^2	RMSE	TP	R^2	RMSE	TP 1	TP 2
Entire study region	0.036	6.051	0.214	0.135	2008	0.266	0.130	2007	2014
Beijing-Tianjin-Hebei	0.001	13.176	0.028	0.167	2001	0.031	0.167	2007	2018
Yangtze River Delta	0.000	6.180	0.134	0.152	2010	0.175	0.148	2008	2014
Pearl River Delta	0.135	7.391	0.266	0.156	2008	0.280	0.154	2005	2013

Triangle of central China	0.035	8.199	0.220	0.130	2012	0.254	0.127	2008	2014
Chengdu-Chongqing	0.099	10.159	0.342	0.113	2010	0.355	0.112	2007	2013
Shandong Peninsula	0.000	8.442	0.078	0.129	2007	0.139	0.125	2003	2016
Weihe Plain	0.010	12.309	0.045	0.111	2014	0.061	0.111	2003	2018
Central Plain	0.004	11.443	0.068	0.100	2014	0.073	0.099	2001	2014

R^2: coefficient of determination; RMSE: root mean squared error; TP: turning point.

Table A2. The collinearity statistics of the MLR model between ground $PM_{2.5}$ and nine selected factors based on the multi-year mean data.

Variables	Relative Humidity	Temperature	Wind Speed	Boundary Layer Height	Builtup Area	Population_Density	GDP_per_Capita	Industry_Ratio	Road_Area
Tolerance	0.16	0.30	0.63	0.24	0.12	0.63	0.74	0.77	0.11
VIF	6.40	3.36	1.59	4.17	8.32	1.59	1.35	1.30	9.15

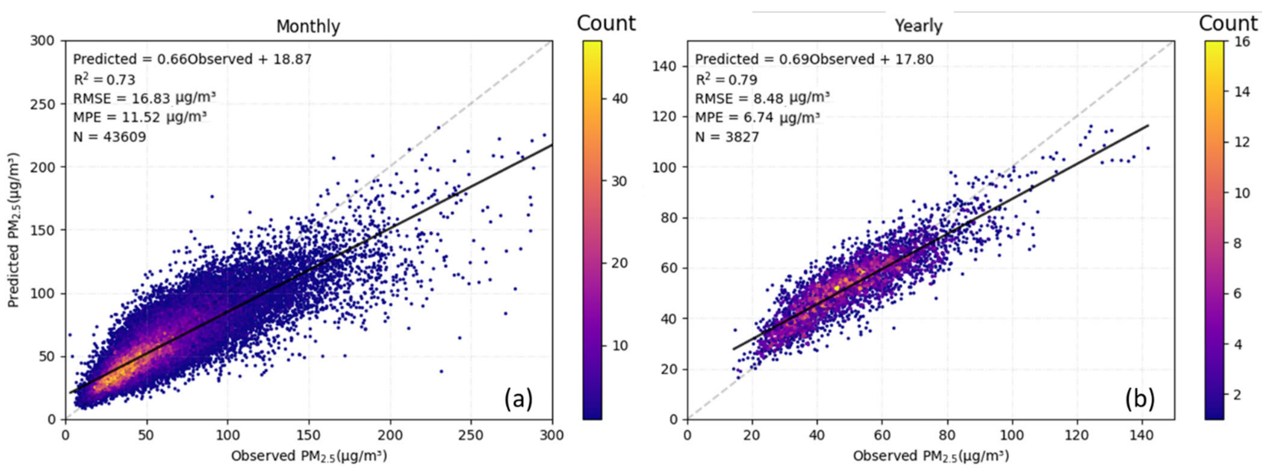

Figure A1. Scatterplot of predicted vs. observed $PM_{2.5}$ concentrations at (**a**) monthly and (**b**) yearly timescales. For the monthly/yearly mean observed $PM_{2.5}$, all records from monitors, i.e., including those grid cells where satellite AOD was not available, were averaged, and only those averaged from more than 5/330 valid daily measurements a month/year remained for evaluation.

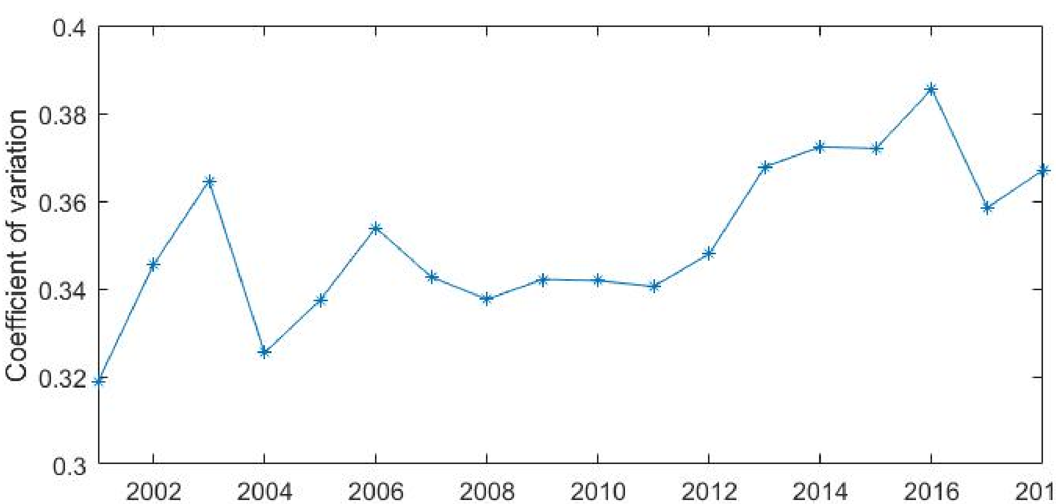

Figure A2. The annual coefficient of variation in $PM_{2.5}$ over eastern China from 2001 to 2018.

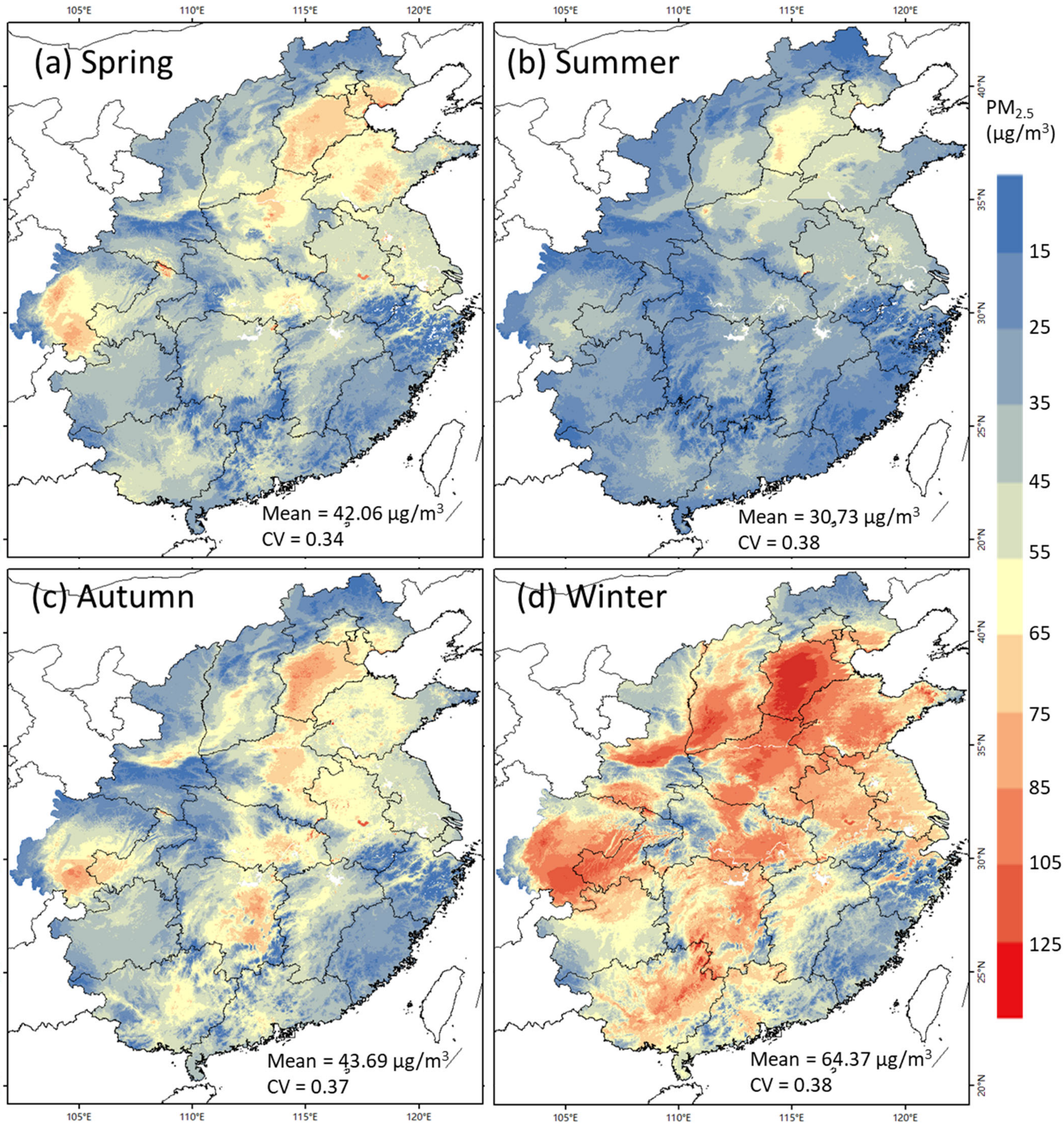

Figure A3. Spatial distributions of seasonal mean $PM_{2.5}$ from 2001 to 2018 (CV represents the coefficient of variation).

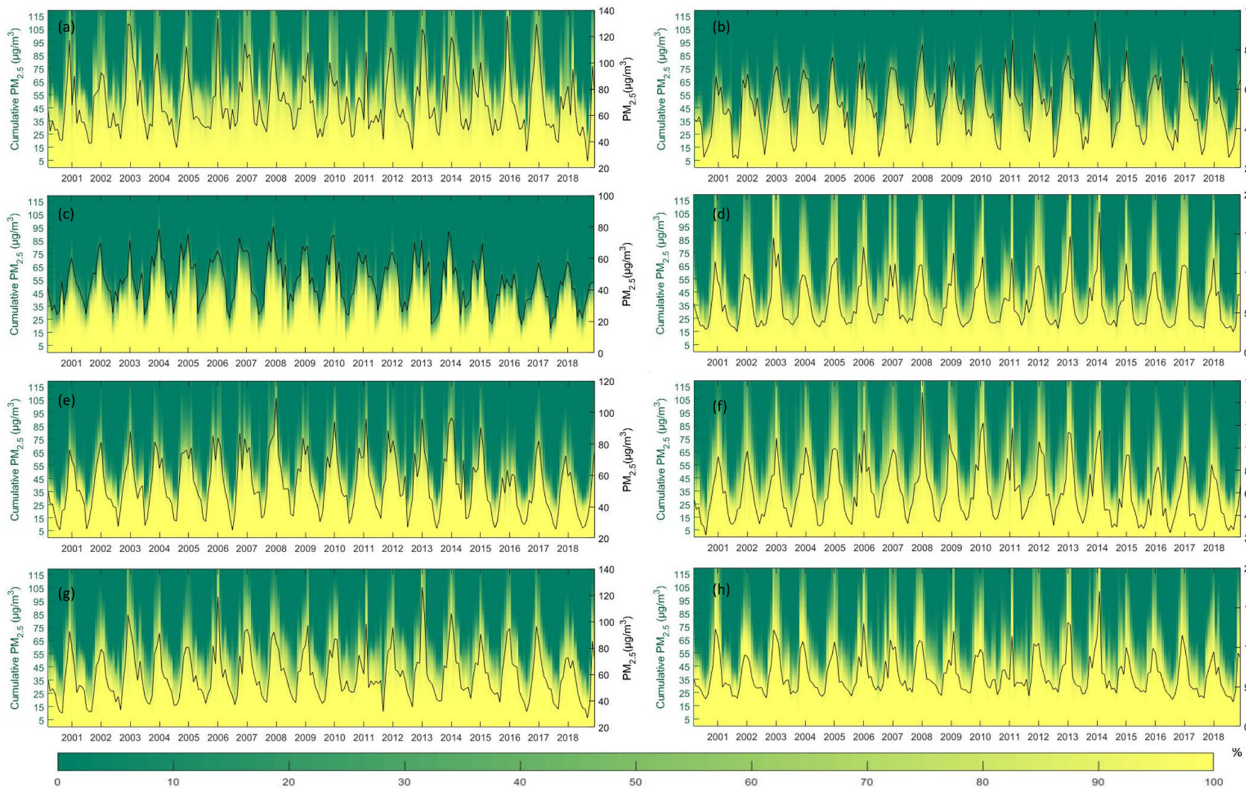

Figure A4. Temporal trends of monthly mean population-weighted $PM_{2.5}$ levels from March 2000 to December 2018 over (**a**) the BTH, (**b**) YRD, (**c**) PRD, (**d**) WHP, (**e**) TCC, (**f**) CDCQ, (**g**) SDP, and (**h**) CP region (the horizontal color bar is the proportion of the population exposed to cumulative $PM_{2.5}$ concentrations (μg/m^3) (left axis), and the solid line and right axis represent the population-weighted $PM_{2.5}$ averages (μg/m^3) over the eight urban regions).

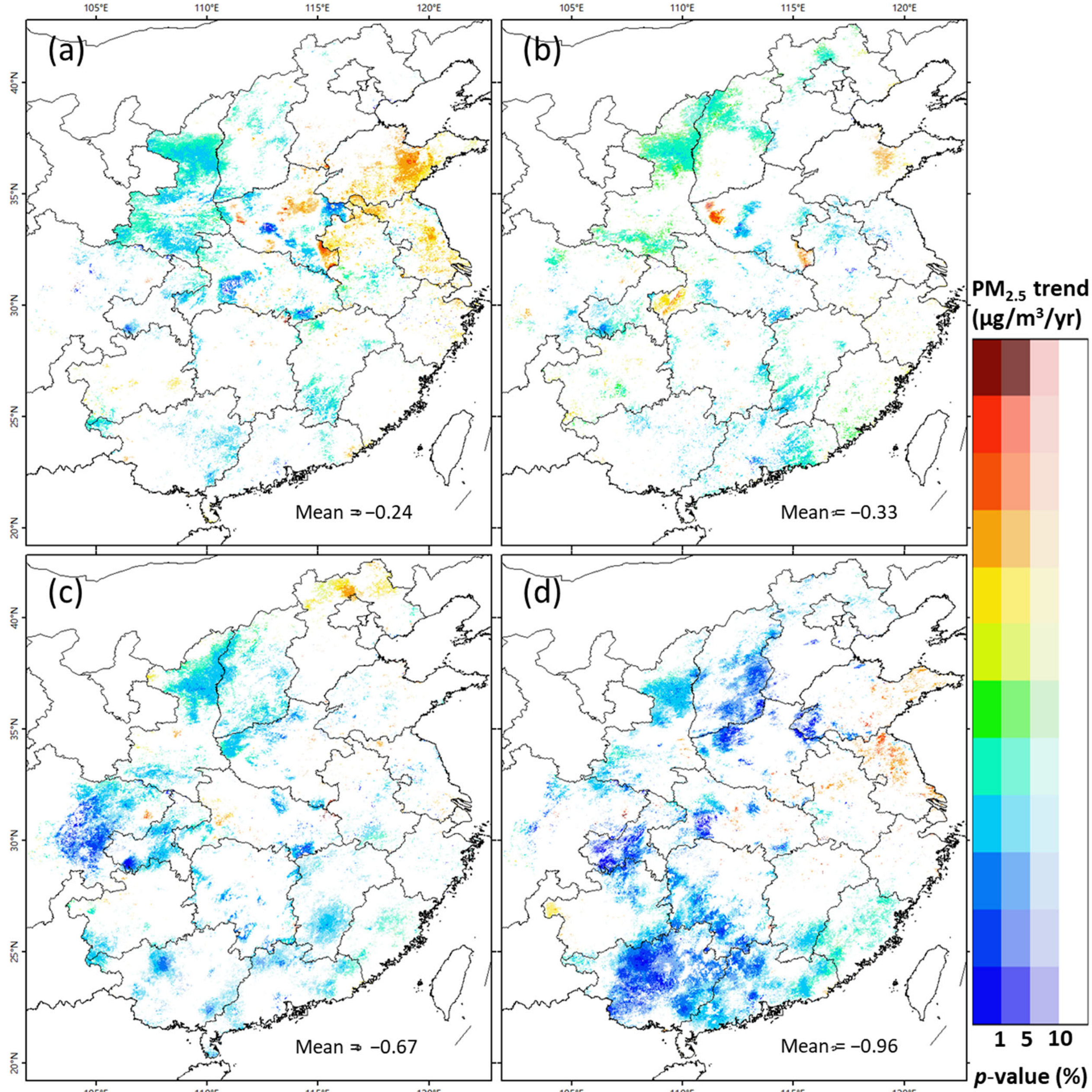

Figure A5. Satellite-derived seasonal linear trends from 2000 to 2018 over the study area using the generalized least-squares regression for (**a**) spring, (**b**) summer, (**c**) autumn, and (**d**) winter. Warm and cold color represents positive and negative trends, respectively; the transparency of colors represents the statistical *p*-value of trends.

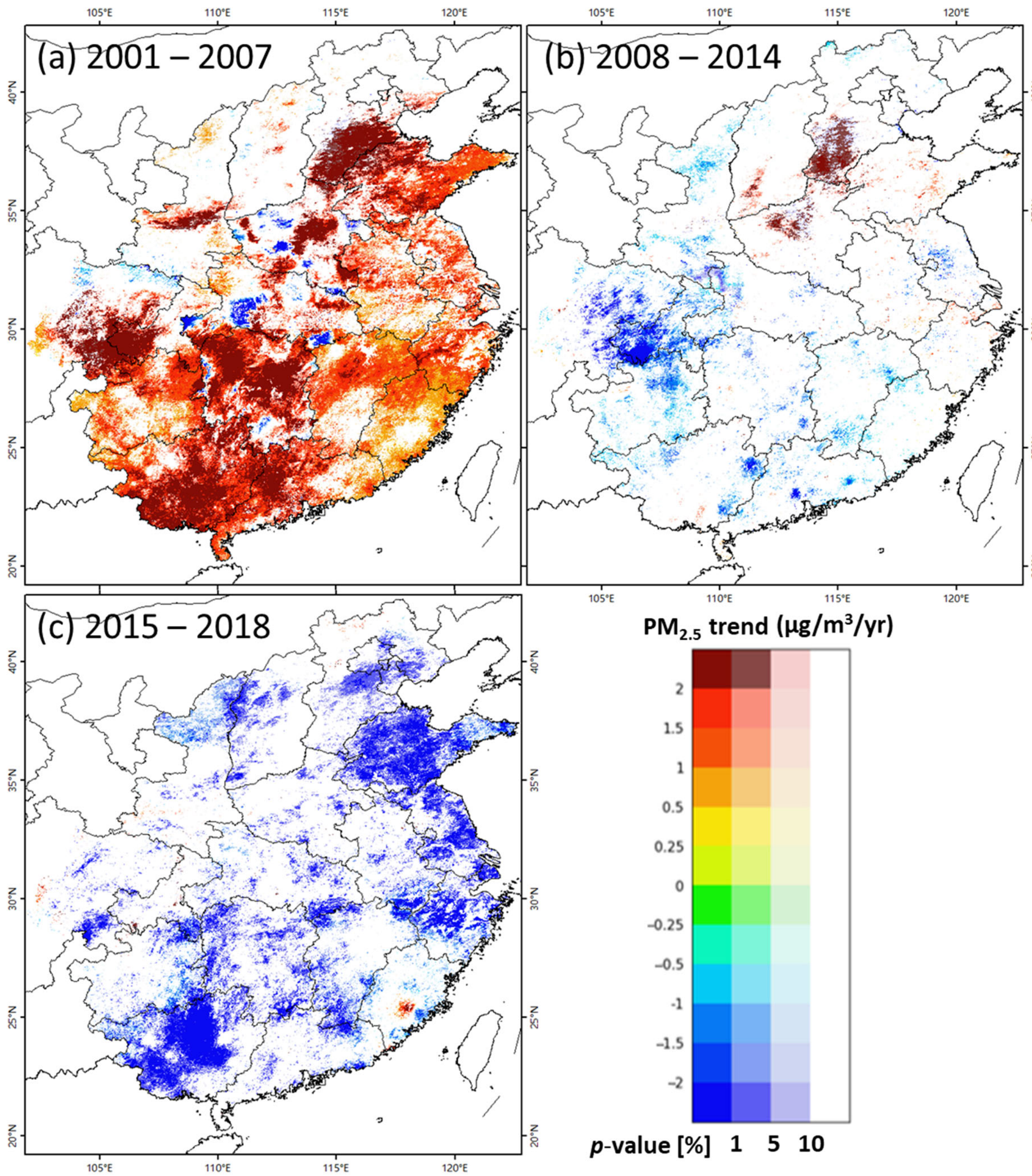

Figure A6. Spatial distribution of linear trends in monthly time series $PM_{2.5}$ anomaly from (**a**) 2001–2007, (**b**) 2008–2014, and (**c**) 2015–2018 periods using the generalized least-squares regression. Warm and cold color represents positive and negative trends, respectively; the transparency of colors represents the statistical *p*-value of trends.

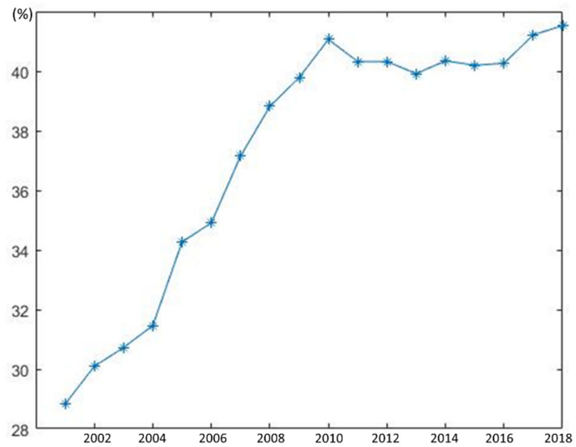

Figure A7. Time series of annual mean green space ratio from 2001 to 2018 in eastern China. Data are from the China City Statistical Yearbook of 2002 to 2019.

References

1. Schwartz, J. Air pollution and hospital admissions for respiratory disease. *Epidemiology* **1996**, *7*, 20–28.
2. Barnett, A.G.; Williams, G.M.; Schwartz, J.; Best, T.L.; Neller, A.H.; Petroeschevsky, A.L.; Simpson, R.W. The effects of air pollution on hospitalizations for cardiovascular disease in elderly people in Australian and New Zealand cities. *Environ. Health Perspect.* **2006**, *114*, 1018.
3. Zhou, M.; Wang, H.; Zhu, J.; Chen, W.; Wang, L.; Liu, S.; Li, Y.; Wang, L.; Liu, Y.; Yin, P.; et al. Cause-specific mortality for 240 causes in China during 1990–2013: A systematic subnational analysis for the Global Burden of Disease Study 2013. *Lancet* **2016**, *387*, 251–272.
4. Cohen, A.J.; Brauer, M.; Burnett, R.; Anderson, H.R.; Frostad, J.; Estep, K.; Balakrishnan, K.; Brunekreef, B.; Dandona, L.; Dandona, R.; et al. Estimates and 25-year trends of the global burden of disease attributable to ambient air pollution: An analysis of data from the Global Burden of Diseases Study 2015. *Lancet* **2017**, *389*, 1907–1918.
5. Guo, J.-P.; Zhang, X.-Y.; Wu, Y.-R.; Zhaxi, Y.; Che, H.-Z.; La, B.; Wang, W.; Li, X.-W. Spatio-temporal variation trends of satellite-based aerosol optical depth in China during 1980–2008. *Atmos. Environ.* **2011**, *45*, 6802–6811.
6. Van Donkelaar, A.; Martin, R.V.; Brauer, M.; Hsu, N.C.; Kahn, R.A.; Levy, R.C.; Lyapustin, A.; Sayer, A.M.; Winker, D.M. Global estimates of fine particulate matter using a combined geophysical-statistical method with information from satellites, models, and monitors. *Environ. Sci. Technol.* **2016**, *50*, 3762–3772.
7. Gui, K.; Che, H.; Wang, Y.; Wang, H.; Zhang, L.; Zhao, H.; Zheng, Y.; Sun, T.; Zhang, X. Satellite-derived $PM_{2.5}$ concentration trends over Eastern China from 1998 to 2016: Relationships to emissions and meteorological parameters. *Environ. Pollut.* **2019**, *247*, 1125–1133.
8. Lin, C.Q.; Liu, G.; Lau, A.K.H.; Li, Y.; Li, C.C.; Fung, J.C.H.; Lao, X.Q. High-resolution satellite remote sensing of provincial $PM_{2.5}$ trends in China from 2001 to 2015. *Atmos. Environ.* **2018**, *180*, 110–116.
9. Ma, Z.; Liu, R.; Liu, Y.; Bi, J. Effects of air pollution control policies on $PM_{2.5}$pollution improvement in China from 2005 to 2017: A satellite-based perspective. *Atmos. Chem. Phys.* **2019**, *19*, 6861–6877.
10. Wang, S.; Zhang, Q.; Martin, R.V.; Philip, S.; Liu, F.; Li, M.; Jiang, X.; He, K. Satellite measurements oversee China' sulfur dioxide emission reductions from coal-fired power plants. *Environ. Res. Lett.* **2015**, *10*, 114015.
11. Ma, Z.; Hu, X.; Sayer, A.M.; Levy, R.; Zhang, Q.; Xue, Y.; Tong, S.; Bi, J.; Huang, L.; Liu, Y. Satellite-based spatiotemporal trends in $PM_{2.5}$ concentrations: China, 2004–2013. *Environ. Health Perspect.* **2016**, *124*, 184–192.
12. Guo, J.; Xia, F.; Zhang, Y.; Liu, H.; Li, J.; Lou, M.; He, J.; Yan, Y.; Wang, F.; Min, M.; et al. Impact of diurnal variability and meteorological factors on the $PM_{2.5}$-AOD relationship: Implications for $PM_{2.5}$remote sensing. *Environ. Pollut.* **2017**, *221*, 94–104.
13. Yang, Q.; Yuan, Q.; Yue, L.; Li, T.; Shen, H.; Zhang, L. The relationships between $PM_{2.5}$ and aerosol optical depth (AOD) in mainland China: About and behind the spatio-temporal variations. *Environ. Pollut.* **2019**, *248*, 526–535.
14. Bian, Y.; Huang, Z.; Ou, J.; Zhong, Z.; Xu, Y.; Zhang, Z.; Xiao, X.; Ye, X.; Wu, Y.; Yin, X.; et al. Evolution of anthropogenic air pollutant emissions in Guangdong Province, China, from 2006 to 2015. *Atmos. Chem. Phys.* **2019**, *19*, 11701–11719.
15. Lin, C.; Lau, A.K.; Li, Y.; Fung, J.C.; Li, C.; Lu, X.; Li, Z. Difference in $PM_{2.5}$ variations between urban and rural areas over eastern China from 2001 to 2015. *Atmosphere* **2018**, *9*, 312.
16. Wang, S.; Zhou, C.; Wang, Z.; Feng, K.; Hubacek, K. The characteristics and drivers of fine particulate matter ($PM_{2.5}$) distribution in China. *J. Clean. Prod.* **2017**, *142*, 1800–1809.
17. Zhou, C.; Chen, J.; Wang, S. Examining the effects of socioeconomic development on fine particulate matter ($PM_{2.5}$) in China's cities using spatial regression and the geographical detector technique. *Sci. Total Environ.* **2018**, *619*, 436–445.

18. Zhang, Y.-L.; Cao, F. Fine particulate matter ($PM_{2.5}$) in China at a city level. *Sci. Rep.* **2015**, *5*, 1–12.
19. Hao, Y.; Liu, Y.-M. The influential factors of urban $PM_{2.5}$ concentrations in China: A spatial econometric analysis. *J. Clean. Prod.* **2016**, *112*, 1443–1453.
20. Yang, Q.; Yuan, Q.; Li, T.; Shen, H.; Zhang, L. The relationships between $PM_{2.5}$ and meteorological factors in China: Seasonal and regional variations. *Int. J. Environ. Res. Public Health* **2017**, *14*, 1510.
21. Hu, J.; Wang, Y.; Ying, Q.; Zhang, H. Spatial and temporal variability of $PM_{2.5}$ and PM_{10} over the North China Plain and the Yangtze River Delta, China. *Atmos. Environ.* **2014**, *95*, 598–609.
22. Ye, W.-F.; Ma, Z.-Y.; Ha, X.-Z. Spatial-temporal patterns of $PM_{2.5}$ concentrations for 338 Chinese cities. *Sci. Total Environ.* **2018**, *631–632*, 524–533.
23. Liu, Q.; Wang, S.; Zhang, W.; Li, J.; Dong, G. The effect of natural and anthropogenic factors on $PM_{2.5}$: Empirical evidence from Chinese cities with different income levels. *Sci. Total Environ.* **2019**, *653*, 157–167.
24. Luo, J.; Du, P.; Samat, A.; Xia, J.; Che, M.; Xue, Z. Spatiotemporal Pattern of $PM_{2.5}$ Concentrations in Mainland China and Analysis of Its Influencing Factors using Geographically Weighted Regression. *Sci. Rep.* **2017**, *7*, 40607.
25. Bai, K.; Ma, M.; Chang, N.B.; Gao, W. Spatiotemporal trend analysis for fine particulate matter concentrations in China using high-resolution satellite-derived and ground-measured $PM_{2.5}$ data. *J. Environ. Manag.* **2019**, *233*, 530–542.
26. Ding, Y.; Zhang, M.; Qian, X.; Li, C.; Chen, S.; Wang, W. Using the geographical detector technique to explore the impact of socioeconomic factors on $PM_{2.5}$ concentrations in China. *J. Clean. Prod.* **2019**, *211*, 1480–1490.
27. He, J.; Gong, S.; Yu, Y.; Yu, L.; Wu, L.; Mao, H.; Song, C.; Zhao, S.; Liu, H.; Li, X.; et al. Air pollution characteristics and their relation to meteorological conditions during 2014–2015 in major Chinese cities. *Environ. Pollut.* **2017**, *223*, 484–496.
28. Vieira-Filho, M.S.; Lehmann, C.; Fornaro, A. Influence of local sources and topography on air quality and rainwater composition in Cubatão and São Paulo, Brazil. *Atmos. Environ.* **2015**, *101*, 200–208.
29. Zhao, X.; Zhou, W.; Han, L.; Locke, D. Spatiotemporal variation in $PM_{2.5}$concentrations and their relationship with socioeconomic factors in China's major cities. *Environ. Int.* **2019**, *133*, 105145.
30. Liu, Q.; Wu, R.; Zhang, W.; Li, W.; Wang, S. The varying driving forces of $PM_{2.5}$ concentrations in Chinese cities: Insights from a geographically and temporally weighted regression model. *Environ. Int.* **2020**, *145*, 106168.
31. He, Q.; Gao, K.; Zhang, L.; Song, Y.; Zhang, M. Satellite-derived 1-km estimates and long-term trends of $PM_{2.5}$ concentrations in China from 2000 to 2018. *Environ. Int.* **2021**, *156*, 106726.
32. Huang, B.; Wu, B.; Barry, M. Geographically and temporally weighted regression for modeling spatio-temporal variation in house prices. *Int. J. Geogr. Inf. Sci.* **2010**, *24*, 383–401.
33. He, Q.; Gu, Y.; Zhang, M. Spatiotemporal trends of $PM_{2.5}$ concentrations in central China from 2003 to 2018 based on MAIAC-derived high-resolution data. *Environ. Int.* **2020**, *137*, 105536.
34. Xue, T.; Zheng, Y.; Tong, D.; Zheng, B.; Li, X.; Zhu, T.; Zhang, Q. Spatiotemporal continuous estimates of $PM_{2.5}$ concentrations in China, 2000–2016: A machine learning method with inputs from satellites, chemical transport model, and ground observations. *Environ. Int.* **2019**, *123*, 345–357.
35. Li, J.; Han, X.; Jin, M.; Zhang, X.; Wang, S. Globally analysing spatiotemporal trends of anthropogenic $PM_{2.5}$ concentration and population's $PM_{2.5}$ exposure from 1998 to 2016. *Environ. Int.* **2019**, *128*, 46–62.
36. Baker, A.; Zalta, E.N. Stanford encyclopedia of philosophy. *Simplicity* 2004.
37. Gauch, H.G., Jr.; Gauch, H.G. *Scientific Method in Practice*; Cambridge University Press: Cambridge, UK, 2003.
38. Weatherhead, E.C.; Reinsel, G.C.; Tiao, G.C.; Meng, X.L.; Choi, D.; Cheang, W.K.; Keller, T.; DeLuisi, J.; Wuebbles, D.J.; Kerr, J.B.; et al. Factors affecting the detection of trends: Statistical considerations and applications to environmental data. *J. Geophys. Res. Atmos.* **1998**, *103*, 17149–17161.
39. Boys, B.L.; Martin, R.V.; van Donkelaar, A.; MacDonell, R.J.; Hsu, N.C.; Cooper, M.J.; Yantosca, R.M.; Lu, Z.; Streets, D.G.; Zhang, Q.; et al. Fifteen-year global time series of satellite-derived fine particulate matter. *Environ. Sci. Technol.* **2014**, *48*, 11109–11118.
40. Charlton, M.; Fotheringham, S.; Brunsdon, C. *Geographically Weighted Regression. White Paper*; National Centre for Geocomputation. National University of Ireland Maynooth: Kildare, Ireland, 2009.
41. Wang, J.; Xu, C. Geodetector: Principle and prospective. *Acta Geogr. Sin.* **2017**, *72*, 116–134.
42. Xiao, Q.; Geng, G.; Liang, F.; Wang, X.; Lv, Z.; Lei, Y.; Huang, X.; Zhang, Q.; Liu, Y.; He, K. Changes in spatial patterns of $PM_{2.5}$ pollution in China 2000–2018: Impact of clean air policies. *Environ. Int.* **2020**, *141*, 105776.
43. Fu, J.; Jiang, D.; Huang, Y. KM Grid Population Dataset of China (PopulationGrid_China). *Glob. Change Res. Data Publ. Repos.* **2014**. https://doi.org/10.3974/geodb.2014.01.06.V1.
44. Jacob, D.J.; Winner, D.A. Effect of climate change on air quality. *Atmos. Environ.* **2009**, *43*, 51–63.
45. Zheng, B.; Tong, D.; Li, M.; Liu, F.; Hong, C.; Geng, G.; Li, H.; Li, X.; Peng, L.; Qi, J.; et al. Trends in China's anthropogenic emissions since 2010 as the consequence of clean air actions. *Atmos. Chem. Phys.* **2018**, *18*, 14095–14111.
46. Wang, Z.-B.; Fang, C.-L. Spatial-temporal characteristics and determinants of $PM_{2.5}$ in the Bohai Rim Urban Agglomeration. *Chemosphere* **2016**, *148*, 148–162.